Random-walk mechanism for step retraction on hydrogen-etched Si(111)

Mats I. Larsson,[*] Heidrun Bethge, Ulrich Köhler,[†] Stefan Menke, and Martin Henzler

Institut für Festkörperphysik, Universität Hannover, Appelstraße 2, D-30167 Hannover, Germany

(Received 3 March 1997)

We report on step retraction on hydrogen-etched Si(111) surfaces. The study was performed by kinetic Monte Carlo simulations and *in situ* high-temperature scanning tunneling microscopy. The origin of the step retraction is the random walk of surface monovacancies. They are caused by desorption of silicon hydrides from the hydrogen-exposed surface, which causes a weak etching effect. The vacancies diffuse until they reach a step or another surface vacancy, where they are annihilated. This results in bilayer step retraction or vacancy cluster coarsening. For sufficiently high temperatures and slow enough etching, all created vacancies reach the terrace steps, which results in maximal step retraction. For sufficiently low temperatures and fast enough etching the step retraction is effectively suppressed by the creation of vacancy clusters in the terraces. For intermediate temperatures and etching, a transition regime is found, where initially all surface vacancies diffuse to the terrace step edges and annihilate. However, the probability for the creation of vacancy clusters in the terraces is not neglectable, so after a widely distributed time a sufficiently large number of monovacancies meet to form a stable vacancy cluster, which effectively slows down the step retraction rate. [S0163-1829(97)08828-0]

Hydrogen interactions with silicon surfaces is of high technological relevance due to the industrial applications of the chemical vapor deposition technique, where silane SiH_4, Si_2H_6, or Si_3H_8 can be used as precursor gases for epitaxial growth.[1] In this work we are going to study the reversed process, i.e., weak etching of Si(111) effectuated by hydrogen-induced desorption of silicon hydrides (SiH_n).[2–6] This is accomplished of hydrogen exposure of the surface at sufficiently high temperatures. Reviews of the field, including lower-temperature properties and characterization of H-induced surface defects, were presented in Refs. 7–11.

Under hydrogen exposure a temperature dependence of the H desorption was reported such that the H desorption from the dihydride and trihydride desorption sites occurs at approximately 410 °C, and the monohydride sites at 540 °C.[12,13] In this context we would like to mention that preferential desorption sites were studied with atomic resolution some decades ago, using replica and transmission electron microscopy techniques.[14]

In this paper we expose a well-prepared Si(111)−7×7 substrate to atomic hydrogen at substrate temperatures higher than the monohydride peak 540 °C. The measurements are performed with high-temperature *in situ* scanning tunneling microscopy (STM).[6] Our experimental results are quantitatively compared with kinetic Monte Carlo (MC) simulations. This type of simulations was recently used to study sputtering of vicinal metal surfaces.[15]

For high enough temperatures or sufficiently slow hydrogen etching, all created surface vacancies are found to reach a step edge, giving rise to maximum bilayer step retraction. For low enough temperatures or high enough hydrogen exposure the majority of the monovacancies encounters other vacancies, and forms vacancy clusters in the terrace and does not reach a step. In this etching regime the step retraction rate R_{step} is very low. For intermediate temperature and etching regimes, there is typically a transition from fast step re-

traction to a slower one due to the formation of vacancy clusters in the terraces after a widely distributed initial time interval.

The experiments were performed in an ultrahigh-vacuum chamber with a base pressure $p < 2 \times 10^{-10}$ mbar. All experiments were performed time resolved and *in situ*. The sample is located inside the scanning tunneling microscope, and images are taken at elevated temperature. This enables us to follow a specific location on the surface through different stages of the etch attack taking sequences of STM images. Bias voltages below 2.2 V and tunneling currents below 1.2 nA are used. *In situ* experiments with atomic hydrogen are performed using a water-cooled H-cracking cell containing a heated tungsten filament pointing under an angle of 15° to the surface at a distance of 8 cm. A direct line of sight between the area imaged in the scanning tunneling microscope, and the source of the atomic hydrogen is needed for *in situ* STM studies. Therefore the STM tip is retracted a few thousand Å between successive images to avoid shading effects. The substrate samples were cut from P-doped Si(111) wafers with high resistivity. In most experiments high precision oriented samples with terrace widths larger than 4500 Å have been used. The samples were prepared in vacuum by carefully outgassing at 600 °C using resistive heating for several hours and subsequently high temperature flashing to 1250 °C. The temperature was measured using an infrared pyrometer.

Si on Si(111) grows in a bilayer mode[16] and we will show in this study that Si can also be etched in a bilayer mode. The bilayer mode comes about because there is one bond to the substrate for adatoms in odd layers and three bonds to the substrate for adatoms in even layers. Unreconstructed Si(111) surfaces are terminated by even layers, which minimizes the surface energy of the system. In our MC model the diamond cubic (dc) structure is modeled by a modified fcc(111) model which phenomenologically takes into account the properties of the dc structure. The adatom hopping

                                       1021

probability is calculated from the initial coordination number n_i, and the final coordination number n_f, of the atoms under interrogation. For the primitive fcc lattice there are in principle 12 different local environments for an atom to diffuse from, depending on the number of nearest neighbors, but we include only up to nine configurations since the probabilities of configurations with higher coordination are extremely low.

To favor the bilayer ordering in our model, the number of nearest neighbors perceived by the adatoms is modified. The optimal bilayer ordering was accomplished by increasing the initial number of atomic bonds for even layers and the final number of atomic bonds for odd layers according to $n_{i,\text{even}} = n_i + 2$ and $n_{f,\text{odd}} = n_f + 4$, respectively. The final number of bonds for even planes and the initial number of bonds for odd planes are not altered, i.e., $n_{f,\text{even}} = n_f$, and $n_{i,\text{odd}} = n_i$, respectively. These modifications strongly improve the adatom mobility in odd planes and stabilize the even crystal planes. This gives a net mass transport upwards over odd-plane step edges, which results in the formation of large even terraces. Overhangs and bulk vacancies are not included into the model.

The simulations are performed on a lattice of dimension $L_x \times L_y$, where $L_x = 64$ and $L_y = 32$ with initially one bilayer step at $L_y = 16$. Although the experiments were performed on much larger surfaces, they, as well as the simulations, were of somewhat stochastic nature. Hence we did not simulate larger systems because any significant improvement seemed impossible to attain without going to very large systems, which could not be done due to computer limitations. Modified periodic boundary conditions were employed normal to steps such that $h(x, L_y + 1) - 2 = h(x, 1)$ and $h(x, 0) + 2 = h(x, L_y)$, effectively giving a start lattice consisting of a 32-lattice-site-wide terrace and one step, where $h(x, y)$ is the height of the lattice site (x, y). Ordinary periodic boundary conditions are used along the x direction, i.e., $h(L_x + 1, y) = h(1, y)$ and $h(0, y) = h(L_x, y)$.

The adatom diffusion is described in terms of hopping rates $\nu_{i,f}$ for an atom at site i to perform a hop to a neighboring site f, and is given by $\nu_{i,f} = \nu_0 \exp[-E(n_i, n_f)/kT]$, where $\nu_0 = 2.7 \times 10^{13}$ s^{-1} is the effective attempt frequency for atomic hopping. k is Boltzmann's constant, T is the substrate temperature, and the activation energy E is given by $E(n_i, n_f) = n_i E_n + (n_i - n_f) E_b$. Note that $E_b = 0$ gives locally isotropic diffusion for atoms at steps; while $E_b \neq 0$ leads to locally anisotropic diffusion where diffusion along steps is easier than diffusion normal to steps. In our model, the ratio $E_n / E_b = 3/2$ was found to give the most excellent bilayer by bilayer growth, and was consequently used to investigate the etching properties. E_n and E_b are fixed to $E_n = 0.23$ eV and $E_b = 0.16$ eV by the relationship $E(n_i, n_f) = T_{\text{expt}} \times [E(n_i, n_f)/T]_{\text{fit}}$, where T_{expt} is the experimental temperature and $[E(n_i, n_f)/T]_{\text{fit}}$ is the best fit value of the simulation. The etching rate at the surface is given by $N_s R$, where N_s is the number of surface sites in the system and R is the etching rate per lattice site.

As the first step of a MC iteration, an etching rate R or a hopping rate $\nu_{i,f}$ is selected randomly with a weighted probability $N_s R / R_{\text{tot}}$ or $N_{i,f} \nu_{i,f} / R_{\text{tot}}$, respectively, where $N_{i,f}$ is the number of rates $\nu_{i,f}$. All rates are summed up in a fixed order to give the total rate of the system $R_{\text{tot}} = N_s R + \Sigma \nu_{i,f}$,
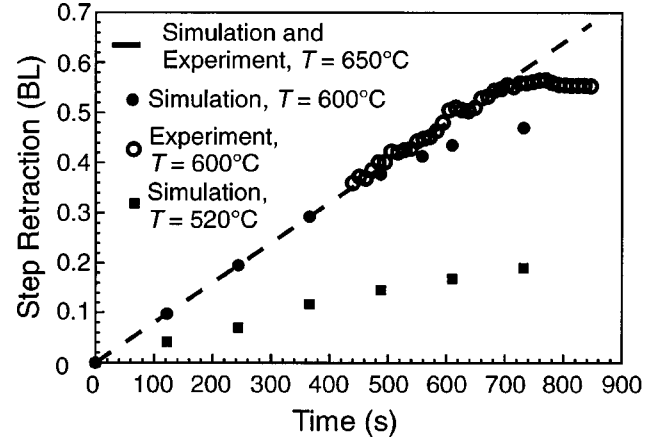

FIG. 1. Step retraction vs time t for the etching rate $R = 8 \times 10^{-4}$ BL/s. In the high-temperature regime exemplified by the temperature $T = 650$ °C, both the simulated and experimental step-retraction rates are given by the maximum value $R_{\text{step}} = 8 \times 10^{-4}$ BL/s, and are described by the dashed line. For intermediate temperatures ($T = 600$ °C was used here), initially the step-retraction rate is give by $R_{\text{step}} = 8 \times 10^{-4}$ BL/s, thereafter the slope levels off. The typical experiment and simulation are denoted by circles and dots, respectively. Step retraction in the low-temperature regime is simulated for $T = 520$ °C, and the data are denoted by filled squares.

where the summation runs over all lattice sites in the system. Second, if a sputtering event is chosen, the most weakly bound adatom in a randomly selected hexagonal surface cell is removed. In case of a diffusion event (specified by the hopping rate $\nu_{i,f}$) a hop from the initial site i to the final site f is performed. The total rate R_{tot} is upgraded after each atomic hop,[17] which takes place with a Poissonian time interval $\Delta \tau = -\ln(r)/R_{\text{tot}}$, where r is a random number in the range $0 < r \leq 1$. The total time is obtained from $t_{\text{tot}} = \Sigma \Delta \tau$.[18] Note, the experimental etching rate R fixes the modeled attempt frequency ν_0, for constant best fit simulated ratio R/ν_0, which defines the time scale $\sim 1/\nu_0$. The correspondence between modeled and experimental time scales are sufficiently good, as will be shown below.

Typical results for our experiments and simulations are shown in Fig. 1, where the etching rate $R = 8 \times 10^{-4}$ BL/s was used. For the highest temperature $T = 650$ °C, the maximum step retraction rate was equal to the total etching rate for both experiments and simulations. The data are described by the dashed curve in Fig. 1. In this temperature regime all etched surface monovacancies reach a step, and no vacancy clusters evolve. For the intermediate temperature $T = 600$ °C, in the beginning all monovacancies encounter a step, giving rise to the maximal step retraction rate, which is shown by dots for the simulation and circles for the experiment. In this regime there is a competing process between vacancy cluster formation and vacancy annihilation at step edges. Thus after an initial time interval of stochastic length, vacancy clusters are formed in the terraces. This process is clearly shown by the simulated surface images in Figs. 2(a)–2(d). The first vacancy cluster is formed after ~ 400 s, and the second after ~ 550 s. Representative STM surface images, obtained for $T = 600$ °C are shown in Figs. 3(a)–3(d) for early times before any vacancy clusters have evolved.

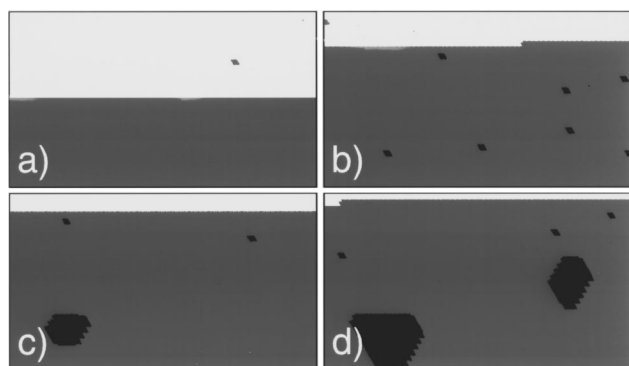FIG. 2. Simulated surface images for the temperature $T = 600\,°C$ and the etching rate $R = 8 \times 10^{-4}$ BL/s. The images were generated at the times (a) $t = 0$, (b) $t = 370$ s, (c) $t = 490$ s, and (d) $t = 610$ s.

Some points on the left-hand side of the terrace are pinned, so it is easy to follow the retraction of the step to the right in the images. Later on, the experimental data (denoted by circles in Fig. 1) levels off to a constant level corresponding to no step retraction. Representative features of a surface in this state of the intermediate etch regime are shown in Figs. 4(a)–4(d) for an experiment performed using the temperature $T = 550\,°C$ and the etching rate $R = 2 \times 10^{-4}$ BL/s. Remarkably, the part of the terrace closest to the step edge is more solid than the interior of the terrace. This is demonstrated in Figs. 4(a)–4(d) by the relatively large white defect-free parts of the step edge, i.e., a partly denuded zone free of vacancies has evolved. This is in strong analogy with the adatom-denuded zones which have been observed in molecular-beam-epitaxy growth experiments. Our observation could be explained by the fact that weakly bound thermally activated
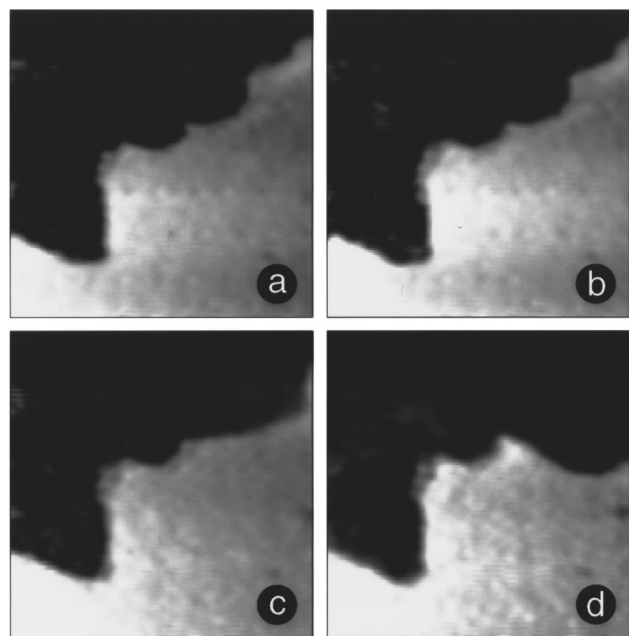

FIG. 3. Experimental surface images of size 500×500 Å^2 for the temperature $T = 600\,°C$ and the etching rate $R = 8.0 \times 10^{-4}$ BL/s for the times (a) $t = 630$ s, (b) $t = 640$ s, (c) $t = 650$ s, and (d) $t = 670$ s.
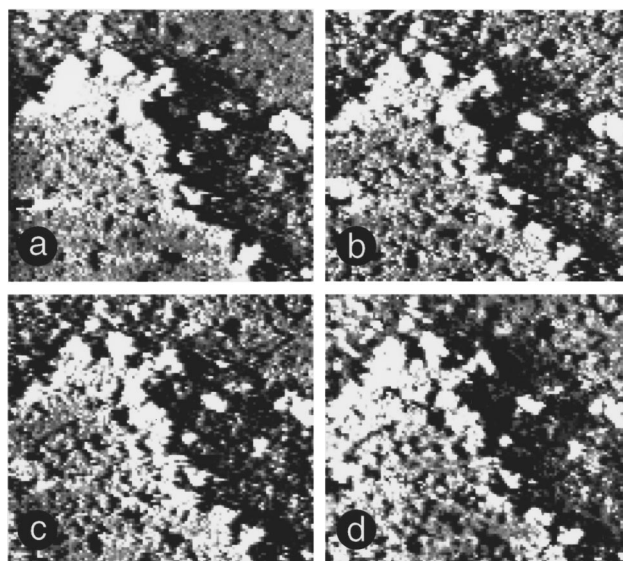
FIG. 4. Experimental surface images of size 840×840 Å^2 for the temperatures $T = 550\,°C$ and the etching rate $R = 2 \times 10^{-4}$ BL/s for the times (a) $t = 840$ s, (b) $t = 1050$ s, (c) $t = 1120$ s, and (d) $t = 1250$ s.

hydrogen adatoms with high probability reach the porous vacancy network in the interior of the terraces where evolution of silicon hydrides is facilitated. This gives rise to a highly reduced etching of the step edge. We would like to point out that the reported mechanism is typical in the intermediate etch regime, although large deviations were observed for which there are many possible explanations, e.g., step meandering and the influences of surface defects. We did not simulate the formation of vacancy-denuded zones (or the effect of surface defects), which explains why the step retraction rate did not level off to zero in the simulation. However, vacancy-denuded zones could most likely be modeled by simply increasing the initial search area used to find the most weakly bound adatom in each etching event.

The lowest-temperature regime, where vacancy clusters are formed from the very beginning, is simulated for $T = 520\,°C$, and is represented in Fig. 1 by filled squares and by the surface images in Figs. 5(a)–5(d). The vacancy clusters are continuously being encountered by diffusing surface
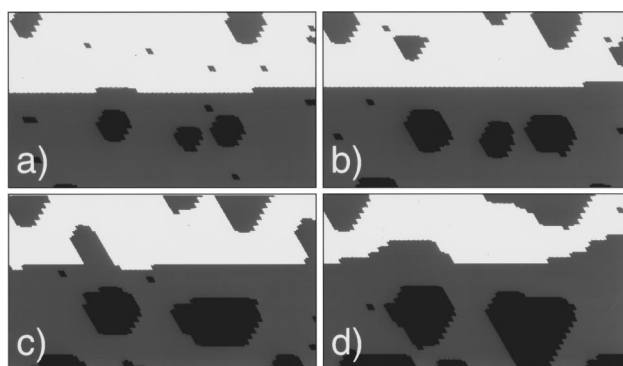

FIG. 5. Simulated surface images for the temperature $T = 520\,°C$ and the etching rate $R = 8.0 \times 10^{-4}$ BL/s for the times (a) $t = 120$ s, (b) $t = 240$ s, (c) $t = 370$ s, and (d) $t = 490$ s.

monovacancies, which annihilate and give rise to the observed coarsening behavior. The slope of the curve shown in Fig. 1 indicates a slow step retraction that can be explained in terms of the limited size of the modeled system, since the rate of step retraction is expected to decrease for increased terrace widths. Experimentally, vacancy kinetics could not be studied unambiguously for the lowest-temperature regime, because the silicon monohydride complexes are stable for $T < 540\,°C$.

To conclude, we have shown that the experimental temperature dependence of the observed step retraction can be excellently explained by kinetic Monte Carlo simulations. Interestingly, the behavior is to a large extent governed by random-walking surface monovacancies, which come about due to weak hydrogen etching of the surface.

---

[*]Also at: University of Karlstad, Department of Natural Sciences, S-65188 Karlstad, Sweden.

[†]Also at: Institut für Experimentalphysik, Universität Kiel, Olshausenstr. 40, D-24098 Kiel, Germany.

[1]S. M. Gates, Surf. Sci. **195**, 307 (1988).

[2]J. Abrefah and D. R. Olander, Surf. Sci. **209**, 291 (1989).

[3]S. M. Gates, R. R. Kunz, and C. M. Greenlief, Surf. Sci. **207**, 364 (1989).

[4]J. B. Boland, J. Vac. Sci. Technol. B **9**, 764 (1991).

[5]M. Ishii, K. Nakashima, I. Tajima, and M. Yamamoto, Jpn. J. Appl. Phys. **31**, 4422 (1992).

[6]U. Köhler, L. Andersohn, and Heidrun Bethge, Phys. Status Solidi A **159**, 39 (1997).

[7]K. Christmann, Surf. Sci. Rep. **9**, 1 (1991).

[8]R. I. G. Uhrberg and G. V. Hansson, Crit. Rev. Solid State Mater. Sci. **17**, 133 (1991).

[9]J. A. Schaefer, Physica B **170**, 45 (1991).

[10]H. Neergaard-Waltenburg and J. T. Yates, Jr., Chem. Rev. **95**, 1589 (1995).

[11]F. Owman, Ph.D. thesis, Linköping University, Sweden, 1996.

[12]M. C. Flowers, N. B. H. Jonathan, Y. Liu, and A. Morris, J. Chem. Phys. **102**, 1034 (1995).

[13]G. Schulze and M. Henzler, Surf. Sci. **124**, 336 (1983).

[14]H. Bethge, Phys. Status Solidi **2**, 3 (1962); **2**, 775 (1962).

[15]P. Šmilauer, M. R. Wilby, and D. D. Vvedensky, Surf. Sci. **291**, L733 (1993).

[16]U. Köhler, J. E. Demuth, R. J. Hamers, J. Vac. Sci. Technol. A **7**, 2860 (1989).

[17]P. A. Maksym, Semicond. Sci. Technol. **3**, 594 (1988).

[18]D. D. Vvedensky and S. Clarke, Surf. Sci. **225**, 373 (1990).